

Structure of Pyridazine in the S_1 State: Experiment and Theory

Doo-Sik Ahn,^[d] Kyo-Won Choi,^[d] Sun Jong Baek,^[d] Young S. Choi,^{*,[a]} Sungyul Lee,^{*,[b]} Heechol Choi,^[c] Kyoung Koo Baeck,^{*,[c]} and Sang Kyu Kim^{*,[d]}

The molecular structure of pyridazine in the first electronically excited state (S_1) is deduced from the combined use of resonance-enhanced two-photon ionization and mass-analyzed threshold ionization spectroscopic methods. The equation-of-motion coupled-cluster single and double (EOM-CCSD) calculation gives the distorted planar geometry for the most stable structure of the S_1 pyridazine. The symmetry constraint of C_{2v} is relaxed to that of

*C_s , and consequently many in-plane vibrational modes are found to be optically active in both S_1 - S_0 and D_0 - S_1 excitation spectra, being appropriately assigned from the comparison of their frequencies with *ab initio* values. This indicates that the S_1 - S_0 excitation is partially localized, and provides an alternative explanation for the long-standing spectroscopic puzzle in S_1 pyridazine.*

1. Introduction

Advances in experimental and theoretical techniques in the last few decades now allow chemists to obtain accurate information for molecules in both the electronic ground and excited states. As quantitative knowledge of molecular structure and dynamics becomes available by using various spectroscopic and quantum-chemical methods, the necessity to generate and employ conceptual tools for qualitatively understanding the problem at hand seems to decrease. The employment of high-level correlated theoretical methods can provide very detailed structures of molecules in the electronically excited state, whereas experimentalists prefer to describe and understand the system using a much simpler molecular orbital view. As Hoffman^[1] stated long ago, however, some old concepts can be very useful for extracting the essence of the phenomena. The concept of orbital interaction is one such example, and it may be instrumental in systematically describing, understanding, and predicting the molecular structure, reaction mechanism, and chemical reactivity.

As applied to the electronic excitation processes, two contrasting and complementary views of orbital interactions were proposed. Diazabenzenes have received a lot of attention as model systems for this situation.^[2-9] In the valence bond (VB) model by Wadt et al.,^[4,5] the excitation is considered to arise from two nonequivalent (and localized) nonbonding orbitals (n_1 and n_2 , the subscripts denoting the two nitrogen atoms), whereas the molecular orbital (MO) view of Hoffman models the process as being from the symmetrized (and delocalized) ground-state nonbonding orbitals ($n_{\pm} = n_1 \pm n_2$). In their analysis of the $^1(n, \pi^*)$ transition of pyridazine, Wadt et al.^[4,5] suggested that studying the two properties (excitation energy and the symmetry of the excited state) may be very useful for determining which viewpoint is more appropriate, and discussed the notion that the MO view may place too much weight on the ionic character in the excited-state wave function, thus predicting too high an excitation energy. By carrying out con-

figuration interaction calculations, they suggested that the VB model is more appropriate.

The electronic delocalization of the nonbonding electron in the excited state of pyridazine may be considered as being relatively weak, and structural distortion due to the local $^1(n, \pi^*)$ excitation has been subsequently suggested to occur by many authors,^[4,8] though its through-bond interaction is known to be significant.^[1] For pyridazine, however, the geometrical distortion in the excited state has hardly been considered to occur, because two closely spaced lone pairs of nitrogen atoms are expected to interact so strongly as to give efficient electronic delocalization (MO model). This conjecture had long been taken for granted, and essentially blocked the investigation of the photophysics and photochemistry of this molecule

[a] Prof. Y. S. Choi
Department of Chemistry
Inha University, Incheon 402-751 (Korea)
Fax: (+82) 32-867-5604
E-mail: yschoi@inha.ac.kr

[b] Prof. S. Lee
School of Environmental Science and Applied Chemistry (BK 21)
Kyunghee University, Kyungki-Do 449-701 (Korea)
Fax: (+82) 31-202-7337
E-mail: sylee@khu.ac.kr

[c] Dr. H. Choi,⁺ Prof. K. K. Baeck
Department of Chemistry
Kangnung University, Gangwon-Do 210-702 (Korea)
Fax: (+82) 33-647-1183
E-mail: baeck@kangnung.ac.kr

[d] D.-S. Ahn, Dr. K.-W. Choi,⁺⁺ Dr. S. J. Baek, Prof. S. K. Kim
Department of Chemistry and School of Molecular Sciences (BK21)
KAIST, Daejeon 301-750 (Korea)
Fax: (+82) 42-869-2810
E-mail: sangkyukim@kaist.ac.kr

[*] Current address:
Department of Chemistry, KAIST, Daejeon 301-750 (Korea)

[++] Current address
Samsung Electronic Company, Cheonan, Choongchung, Nam-Do (Korea)

for last several decades. Even the vibronic assignment in the S_1 - S_0 excitation spectrum had been controversial for a long time in spite of numerous previous spectroscopic works.^[3,6-15] Although Fischer and Wormell made a nice interpretation of previous experimental work in terms of a vibronic coupling model,^[6] several parameters in the model were adjusted in a semiempirical way rather than by exact theoretical computations. The vibronic model is also based upon assumptions, that is, the efficient electronic delocalization and the resulting C_{2v} symmetry of the excited S_1 state. In spite of their apparent successful interpretation of many of the experimental observations, their vibronic coupling method was not rigorous enough to rule out the possibility of alternative successful models for the experimental spectra.

Quite recently, we briefly reported that the pyridazine molecule adopts the distorted planar geometry in the first electronically excited state,^[16] which indicates that the simple MO view and previous theoretical interpretations based on the assumption of C_{2v} symmetry of the S_1 state are not appropriate for the excited pyridazine either. Herein, we present further experimental and theoretical details for elucidating the nature of the excitation and ionization of the pyridazine molecule.

2. Results and Discussion

2.1. S_1 - S_0 and D_0 - S_1 Spectra of Pyridazine

The resonance-enhanced two-photon ionization (R2PI) spectrum of pyridazine is shown in Figure 1a. Assignment of vibronic bands above the origin, however, has never been fully

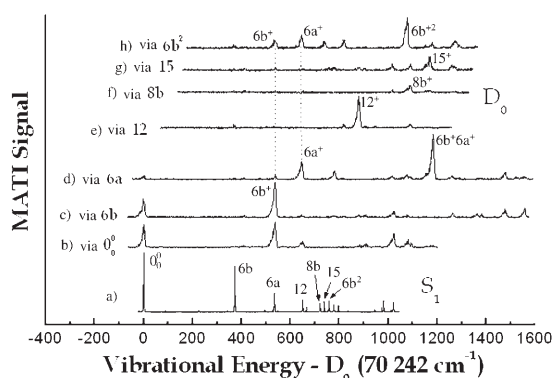


Figure 1. R2PI and MATI spectra taken via various S_1 intermediate states. For the R2PI spectrum, the energy is above the S_1 - S_0 origin at $26\,656\text{ cm}^{-1}$, while the MATI spectra are scaled with respect to the ionization energy at $70\,242\text{ cm}^{-1}$.

or consistently accomplished so far. This is because there has been a long controversy about the nature of a strong band located at 373 cm^{-1} above the S_1 origin. In many previous publications, the 373 cm^{-1} band was ascribed to the origin of a nearby S_2 state, while it was claimed to be due to overtone bands of S_1 in many other works.^[3,6-15] This confusion on the vibronic structure of the excited pyridazine arises from the fact that the interpretations in previous publications were mostly

based on the assumption that the symmetry of the excited pyridazine remains C_{2v} . In a recent publication, we have shown that the excited pyridazine actually belongs to C_s rather than C_{2v} symmetry as a consequence of the local excitation.^[16]

Spectroscopic characterization of the electronically excited state can greatly benefit from mass-analyzed threshold ionization (MATI) spectroscopy, since its successful interpretation of the cationic ground state gives direct information about the vibrational character in the S_1 intermediate state, which is used in the $(1+1')$ MATI excitation scheme. We employ the following strategy for the assignment. In Figure 1b-h, MATI spectra taken from various intermediate S_1 vibronic states are presented to give highly resolved vibronic features of pyridazine in the D_0 state. The ab initio [UB3LYP/6-311+G(d,p); Gaussian98]^[17] calculation for the D_0 pyridazine is carried out to properly assign the vibrational bands observed in the MATI spectra. Then, the S_1 vibronic states are reversely assigned using the fact that the strongest band in each MATI spectrum, following the Franck-Condon principle, represents a vibrational mode of the S_1 state used as an intermediate state for the $(1+1')$ MATI spectrum (Figure 1). The 373 cm^{-1} band turns out not to be the S_2 origin, because then it would be expected that the origin band would be more intense in the MATI spectrum in Figure 1c than the $6b^+$ band located at 537 cm^{-1} above the ionization threshold of $70\,242\text{ cm}^{-1}$. Thus, the 373 cm^{-1} band should be the $6b$ mode of the S_1 state. Were the symmetry of the S_1 pyridazine C_{2v} however, the transition would be forbidden because the vibrational symmetry of $6b$ is b_{2v} while the symmetries of the transition dipole moment and S_1 state are both B_1 in C_{2v} . Therefore, only the reduction of the symmetry species of the 373 cm^{-1} band to A'' in C_s , isomorphic to B_1 in C_{2v} can explain the experimental observation, which means the structural distortion of pyridazine in S_1 . The large intensity enhancement of the combination $6b^+6a^+$ band in the MATI spectrum, taken via the $6a$ mode of S_1 as an intermediate state, also supports the in-plane structural distortion of the S_1 pyridazine, as it is well known that both neutral and cationic ground states belong to the C_{2v} symmetry.^[17] The $6b^+$ band excitation in the MATI spectrum taken via the S_1 - S_0 origin (Figure 1b) should reflect the structural change of the distorted planar geometry of S_1 to the C_{2v} planar structure of D_0 .^[17] Assignments for other strongly observed bands in R2PI and MATI spectra have been straightforwardly done with the help of ab initio calculations, and described in our former publication.^[16] For example, the 758 cm^{-1} band of S_1 correlates to the 1078 cm^{-1} band of D_0 , which indicates that these bands are due to the $6b^2$ (S_1) and $6b^{2+}$ (D_0) modes, respectively. This is the first reliable assignment of the vibronic bands in the S_1 - S_0 excitation spectrum of pyridazine.

We have also measured the rotational contours of all bands in the R2PI spectrum taken at 3 K (Figure 2). All vibronic bands including the origin, 373 ($6b$), and 534 cm^{-1} ($6a$) are found to be almost identical and belong to the C-type transition, as clearly demonstrated in the simulation (Figure 2). This is also consistent with the theoretical transition dipole moment for the S_1 - S_0 transition (see below) which is perpendicular to the molecular plane. The experimental observation indicates that

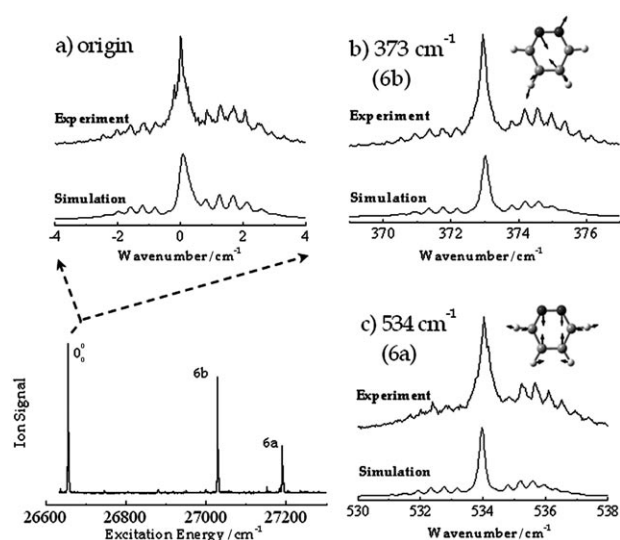


Figure 2. Rotational contours for the a) origin, b) 373 cm^{-1} (6b), and c) 534 cm^{-1} (6a) bands in the S_0 - S_1 R2PI spectrum. In each case, the upper trace is the experiment while the lower trace represents the simulation. All the simulations are for the C-type transition at 3 K. Nuclear displacement vectors are depicted for 6b and 6a modes.

the observed bands have indeed the same a' vibrational symmetry, since the transition dipole moment is perpendicular to the molecular plane (A'') while the S_1 state has the A'' symmetry. This experimental observation provides good evidence that all the observed bands are in the same electronic excited state.

2.2. Ab Initio Calculations for S_1 Pyridazine

Most of the previous work on the $^1(n,\pi^*)$ transition of pyridazine tried to explain the process by using the qualitative concept of orbital interaction, by using two contrasting and complementary viewpoints based upon the VB and MO theories. Once a theoretical calculation goes beyond the independent particle model, such as the VB and MO methods, however, the concept of orbital interaction smears out into the concept of the electronic correlation effect. When the electron correlation effect is properly included, the quantitative results do not depend on the starting independent particle model any more. Then the final result with a high-level theory of electronic correlation could be reinterpreted by using either of the independent particle models. Thus, the use of high-level theoretical methods seems to be an indispensable requirement for the proper quantitative and qualitative theoretical analysis of the $^1(n,\pi^*)$ transition of pyridazine.

Almost all of the previous theoretical work on S_1 pyridazine with high-level electronic structure theories,^[6-15] including multireference configuration interaction (MRCI), equation-of-motion coupled-cluster singles and doubles (EOM-CCSD), EOM-CCSD with noniterative triples [EOM-CCSD(T)], and complete active space with second-order perturbation theory (CASPT2), was well summarized by Fischer and Wormell^[6] with their own theoretical results. They also compared the theoretical vertical and adiabatic excitation energies with the corresponding experimental values. None of the previous theoretic

cal work, however, extensively studied the possibility of a distorted stationary structure of the S_1 pyridazine. Fischer and Wormell found that neither 1B_1 nor 1A_2 corresponds to the true stationary point of the S_1 state. However, they passed on to the vibronic coupling model restricted within the C_{2v} structure just after mentioning that the inversion barrier along the out-of-plane distortion or the twist mode along the C_2 axis is smaller than or comparable to the zero-point vibration energy. As will be shown below, the in-plane distortion suggested by our experimental results provides a new alternative picture of excited S_1 pyridazine.

To generate a full set of information, such as vertical excitation energies, symmetry, structures, and vibrational frequencies, we employ the coupled-cluster singles and doubles (CCSD)^[18] and the EOM-CCSD^[19] methods for the ground and excited electronic states, respectively. All of theoretical calculations in this work are carried out by using the ACES2 program.^[20] The six innermost core molecular orbitals (MOs), corresponding to the 1s atomic orbital (AO) of two N and four C atoms, are dropped, but all of the virtual MOs are included in the post-Hartree-Fock calculations. The analytical gradient methods^[21,22] for the CCSD and EOM-CCSD energies have been extended to handle the cases with frozen MOs, as has been described elsewhere.^[23,24] Most of our CCSD and EOM-CCSD results are computed by using the binary basis sets (Basis-1: 6-31 + G^* on N and C, 6-31G on H). When the geometry of pyridazine has no symmetry element, encountered in the calculation of unsymmetrical vibrational frequencies of the excited state in C_s symmetry, the CCSD and EOM-CCSD computations with Basis-1 become prohibitive due to the huge size of memory required. The vibrational frequencies in those cases are computed with the smaller basis set (Basis-2: 6-31G* for all atoms) after the molecular structures are optimized again with Basis-2. To provide another viewpoint of theoretical calculation, we also carried out similar calculations with the CASSCF(4,4)/6-31 + G^* method implemented in the Gaussian 98 program.^[25]

2.3. Theoretical Structure of S_1 pyridazine

The main results of our calculations are summarized in Table 1, and the energetic relationship among some important saddle and stationary points of the potential energy surface (PES) on the excited S_1 state is depicted in Figure 3. The electronic states obtained by optimization within the symmetry shown in parentheses are represented by horizontal solid bars, whereas the nearest singlet electronic state (S_2) calculated by the single-point EOM-CCSD energy computation at the geometry is given by the horizontal dotted bar just above the state. The energies of the two states (B_1 and A_2) in the leftmost part of Figure 3 are the results of single-point computation at the optimized geometry of the ground state.^[26]

Vertical excitation energies of the two lowest singlet states, the B_1 and A_2 states, are found to be 33267 cm^{-1} (4.125 eV) and 37926 cm^{-1} (4.702 eV), respectively, from the CCSD/EOM-CCSD calculation. The values are comparable with previous theoretical results from similar high-level theories of electronic

Table 1. Relative energies [cm^{-1}], bond lengths [pm], bond angles [$^\circ$], twist angle [$^\circ$], and low vibrational frequencies [cm^{-1}] of S_1 pyridazine.							
Basis set		S_1 /EOM-CCSD(CASSCF) ^[a]				Exp. ^[f]	
		B_1 (C_{2v}) Basis-1	B (C_2) ^[b] Basis-1	A_2 (C_{2v}) Basis-1	Basis-2		A'' (C_s) Basis-1
Relative energy ^[c]		30 508	30 390	30 200	30 683 ^[c]	27 553 ^[c]	
Bond length	$R(\text{C4}-\text{C5})$	146.0	145.6	136.1	140.1	140.6 (143.0)	
	$R(\text{C}-\text{C})$ ^[d]	137.8	137.7	145.8	138.1	138.0 (135.0)	
	$R(\text{C}-\text{N})$ ^[d]	136.0	136.6	136.2 (132.0)	145.4	145.2 (136.0)	
	$R(\text{N1}-\text{N2})$	127.3	127.6	122.0 (123.0)	142.5	142.5 (138.3)	
Bond angle	$A(\text{C}-\text{C}-\text{C})$ ^[d]	118.3	118.4	120.7	123.0, 116.3	122.8, 116.2	
	$A(\text{C}-\text{N}-\text{N})$ ^{[d][g]}	123.3	121.7	126.7	116.4, 114.6	116.6, 114.8	
	$A(\text{C}-\text{C}-\text{N})$ ^[d]	118.3	117.4	112.6	117.7, 132.2	117.6, 132.1, (108.1, 134.7)	
Vibrational frequencies		353 (b_1)	274i (b)	194i	303 (a'')		
		184 i (a_2)	237 (a)	198 i	399 (a'')		
		590 i (b_2)	312 (b)	176 i	296 (a')	335	373 (6b)
		683 (b_1)	680 (b)	389	419 (a'')		
		371 (a_2)	483 (a)	497	506 (a'')		
		572 (a_2)	629 (a)	546	611 (a'')		
		660 (a_1)	659 (a)	608	609 (a')	605	534 (6a)
		597 (b_2)	753 (b)	673	726 (a')	728 ^[e]	650 (12)
		877 (b_1)	861 (b)	706	891 (a')		
		887 (a_2)	868 (a)	850	733 (a'')		

[a] Some results by the CASSCF(4,4)/6-31+G* method are given in parentheses. [b] The twist angle is 12.0° . [c] The relative energy with respect to the ground state. The calculated total energies are -263.37450 , -263.35796 , and -262.45222 Hartrees by the EOM-CCSD/Basis-1, EOM-CCSD/Basis-2, and CASSCF(4,4)/6-31+G* methods, respectively. The adiabatic excitation energies (without zero-point energy correction) of the three methods are 27 553, 30 683, and 27 019 cm^{-1} , respectively. [d] The C_2 structure has two values of the geometrical parameters, the left and right sides, respectively. [e] Other vibrational frequencies of the a' mode by the EOM-CCSD/6-31+G* method are 872, 973, 1025, 1116, 1239, 1268, 1357, 1467, 1511, 1635, 3199, 3249, 3272, and 3303 cm^{-1} , whereas the four lowest frequencies by the CASSCF(4,4)/6-31+G* method are 176, 472, 612, and 616 cm^{-1} . [f] The present work.

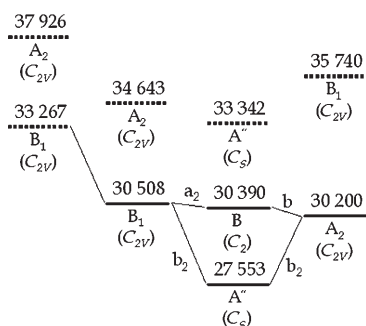


Figure 3. Relative energies (in cm^{-1}) of various local structures of S_1 and S_2 pyridazine with respect to the S_0 state.

correlation.^[6–14] Firstly, we optimized the geometry of the S_1 pyridazine in the B_1 state by imposing the C_{2v} symmetry. The total electronic energy in this case is stabilized by 2759 cm^{-1} in the optimization process. Meanwhile, the energy of the S_2 state (A_2) is computed to be 4135 cm^{-1} higher than that of the B_1 state at the same geometry, as had been reported earlier.^[10] As shown in Table 1, the main changes in the molecular structure of the B_1 state in the restricted optimization include the decrease of the N–N distance and increase of the C–C distance on the opposite side of the N–N moiety.

The calculated vibrational frequencies of this structure, however, exhibit two imaginary frequencies for 6b (b_2) and 16a (a_2)

vibration modes. This implies that the minimum energy geometry of pyridazine in the S_1 electronic state has to be distorted along both the unsymmetrical in-plane (b_2 , 590 i cm^{-1}) and out-of-plane (a_2 , 184 i cm^{-1}) modes. The large imaginary frequency of the b_2 mode strongly supports our experimental findings that pyridazine, despite its strong orbital interaction, could generate two nonequivalent nitrogen atoms in the S_1 state. The a_2 mode, on the other hand, twists the molecule along the C_2 axis and generates two equivalent nitrogen atoms.

To see the influence of the twisting mode, the saddle point of B_1 in C_{2v} is relaxed along the a_2 mode, optimized by imposing just the C_2 symmetry, and converted into the B state in the C_2 symmetry (Figure 3). The optimization lowers the energy of B_1 by just 118 cm^{-1} . The change in the molecular geometry in the optimization is negligible (Table 1), except for the fact that the molecular plane is slightly twisted along the C_2 axis bisecting the molecule through the center of two adjacent N atoms. The twist angle is about 12° . Since the calculated frequencies of the B state in C_2 symmetry include one imaginary value of 274 i cm^{-1} for the b mode, the geometry of the B state is relaxed again along this vibrational mode. The energy of S_1 (B in C_2) is lowered further by 190 cm^{-1} in the optimization process, and yet, interestingly, the optimization ends up with a structure having C_{2v} symmetry with the A_2 state, as given in Table 1 and Figure 3. The N–N distance of 122 pm in A_2 is found to be

even shorter than that of 127 pm in B_1 . The other noticeable change can be found in the shortened C–C distance on the opposite side of the N–N bond compared to that in the ground state,^[26] whereas other bonds of the ring are slightly enlarged. The nearest excited S_2 state at this geometry is the B_1 electronic structure, which lies at 5540 cm^{-1} above the S_1 of A_2 (Figure 3).

When the 1A_2 state is directly optimized starting from the geometry of ground-state pyridazine with the constraint of C_{2v} symmetry, exactly the same geometry of the relaxed 1A_2 state given in Table 1 is obtained. The electronic states represented by horizontal bars in Figure 3 are directly connected by the restricted optimization along the thin lines, whereas the electronic states shown by the horizontal dotted bars are not directly connected to each other. Because the energy gap between S_2 and S_1 is much smaller than the gap between S_1 and S_0 , the study of the interrelationship among many stationary and saddle points of S_2 is always much more difficult than the corresponding study for the S_1 state. The small energy gap between S_2 and S_1 implies many possible conical intersections and almost no S_2 – S_0 fluorescence, as stated by Kasha's rule with very few exceptions.^[27] Although the search for conical intersections between the S_1 and S_2 states of polyatomic molecules is always an interesting and challenging subject, it is not explored further in the present work.

The calculation of the vibrational frequencies of the optimized A_2 in C_{2v} however, produces three imaginary values for b_1 (194i), b_2 (176i), and a_2 (198 i cm^{-1}) modes. The b_1 mode corresponds to the motion of two N atoms out of the molecular plane in the same direction, which would give the C_s symmetry where the symmetry plane bisects the molecular plane. Further optimization of the stationary geometry of the S_1 (A_2) structure along the a_2 or b_1 mode gives the 1A state in C_2 or $^1A''$ in C_s symmetry, respectively. However, their corresponding energies are only 6 (1A) or 40 cm^{-1} ($^1A''$) below the energy of the planar 1A_2 state. The small imaginary frequencies and almost negligible barriers along the a_2 and b_1 modes imply that the PES is virtually planar around the saddle point of A_2 in C_{2v} . It corresponds to the conjecture of Fischer and Wormell^[6] when they proceed to the vibronic coupling model.

Interestingly, when both B_1 and A_2 planar structures are relaxed along the in-plane unsymmetrical b_2 mode, the same final stationary structure of S_1 is obtained. The lower middle part of Figure 3 has to be carefully understood. The picture does not mean the splitting of 1B_1 (or 1A_2) into 1B and $^1A''$. Both 1B and $^1A''$ are connected to 1B_1 (or 1A_2), and yet along different paths of geometrical change. The relationship among the four points (1B_1 , 1B , $^1A''$, and 1A_2) has to be understood as four points in a multidimensional space.

Importantly, the A_2 and B_1 states belong to A'' and A' in C_s , respectively, where the symmetry plane bisects the molecular plane. However, as the molecule is distorted within the molecular plane along the b_2 (6b) vibration mode, two states are found to be reduced to the same A'' electronic state where the molecular plane is the C_s symmetry plane this time. The energy of the final stationary structure is 2647 cm^{-1} below the planar A_2 state. The EOM–CCSD adiabatic excitation energy of

the A'' state is calculated to be 27553 cm^{-1} , which is very close to our experimental value of 26650 cm^{-1} . Virtually the same structure and similar adiabatic excitation energy (27019 cm^{-1}) could also be obtained from the CASSCF(4,4)/6-31 + G* computations, as given in footnote c of Table 1.

The calculation of vibrational frequencies for the A'' state in C_s with the CCSD/EOM–CCSD method requires a huge amount of memory, and the calculation of the geometry optimization and vibrational frequencies of the B state in C_2 are carried out again using Basis-2. The optimization gives almost the same geometry as that obtained with Basis-1 (Table 1). Calculations using Basis-2 provide positive values for all vibrational frequencies, which confirms that the in-plane distorted A'' structure is a true stationary point of the S_1 pyridazine. The three lowest in-plane (a' mode) vibrational frequencies of A'' , computed by using the EOM–CCSD method with the original binary basis sets, are 335, 605, and 728 cm^{-1} , which are comparable to the experimentally observed values of 373, 534, and 650 cm^{-1} , respectively. Other in-plane vibrational frequencies are calculated to be 872, 973, 1025, 1116, 1239, 1268, 1357, 1467, 1511, 1635, 3199, 3249, 3272, and 3303 cm^{-1} .

Our theoretical calculations for the optimized geometry, energy, and vibrational frequencies of the S_1 pyridazine are fully consistent with experimental observations described earlier. As mentioned in our previous brief report, the results clearly suggest that pyridazine adopts an in-plane distorted C_s structure in its first excited state. The agreement between our theoretical vibrational frequency of S_1 pyridazine and the corresponding experimental value is not perfect yet, partially due to small one-electron basis sets. The effect of the triple excitation operator of the EOM–CCSD(T) theory could be part of the deficiency in our computed results. In spite of the limitation, the present theoretical results show that the A_2 and B_1 in C_{2v} are connected by pseudo-rotation along the b_2 and a_2 vibration modes. Therefore, the controversial issue regarding the symmetry of two nearby electronic states, the S_1 (B_1 and A_2), are clearly resolved, since both B_1 and A_2 in C_{2v} correspond to the same A'' state in C_s . The true S_2 state locates at about 4000 – 5000 cm^{-1} above the S_1 state, as mentioned earlier by Terazima et al.^[10]

The vibronic coupling model of Fischer and Wormell was able to generate a very successful interpretation of all previous experimental spectra over wide range of excitation energy.^[6] The success partially depends on careful and semiempirical selection of parameters in the model, such as the energy gap, the vibronic coupling constant, and even the vibrational frequencies for 6a (a_1) and 6b (b_2) modes. Our present theoretical work is much more straightforward, and provides another intuitive and clearer explanation for the vibronic coupling model. Our theoretical computations demonstrate that the energy of the optimized S_1 state with C_s symmetry is about 3000 cm^{-1} below the saddle points in C_{2v} symmetry. Although the zero-point vibration energy of S_1 pyridazine is larger than the inversion barrier between the pseudo-double minimum along the 6b (b_2) mode, the barrier is much larger than a few quanta of the vibration along the 6b (b_2) mode. The vibronic states of S_1 pyridazine with small vibrational quanta, therefore,

may have to be interpreted in terms of the picture provided by our present work, whereas those with larger vibrational quanta and a combination of different vibration modes should be interpreted in terms of the vibronic coupling model of Fischer and Wormell.^[6]

2.4. Comparison with Other Experimental Studies

There have been a number of spectroscopic studies to clarify the nature of the $+373\text{ cm}^{-1}$ band in the excitation spectrum of pyridazine. We do not intend to review all of those studies. Rather, we try to explain some of the previous experimental findings with the model suggested in this work. First of all, Fischer and Wormell^[6] reported that the origin and 373 cm^{-1} band in the S_0 – S_1 absorption spectrum belong to different symmetries based on their different rotational contours. As described above, from the highly resolved rotational contour analyses in this work, all vibronic bands including the origin, 373 (6b) , and 534 cm^{-1} ($6a$) are found to belong to the same vibrational symmetry. The large negative inertial effect reported earlier for the 373 cm^{-1} band^[28] could not be observed in the present work, though a higher-resolution study is desirable for the further resolution of this issue.

The single vibronic-level fluorescence (SVLF) spectra from the origin and 373 cm^{-1} bands of pyridazine are known to be similar.^[12,29] This could happen if the S_0 – S_1 electronic transition is accompanied by a large shift of the vibrational frequency for the same mode, as has been pointed out earlier.^[12] Indeed, the $6b$ mode frequency in S_0 is 629 cm^{-1} ,^[6] which is much larger than the corresponding frequency of 373 cm^{-1} in S_1 . For the same reason, in the MATI spectra where the S_1 – D_0 transition is involved, the large frequency shift from 373 to 537 cm^{-1} gives a different but somewhat similar pattern of two MATI spectra taken via the origin and 373 cm^{-1} band. However, it is quite clear that the signal intensity of the $6b^+$ band is certainly much enhanced by the excitation of the 373 cm^{-1} band of S_1 , which supports the idea that the 373 cm^{-1} band in S_1 has vibrational quanta in the $6b$ mode. The low barrier with respect to the in-plane-distortion $6b$ mode in S_1 may be responsible for the lower activation of the corresponding mode in S_0 and D_0 .

The shift of vibrational frequency is strongly mode-dependent in the matrix. Therefore, the blue shift of the 373 cm^{-1} band as a $6b$ mode^[12] is plausible, since its nuclear displacement associated with the in-plane ring distortion can be easily restricted by the surrounding solvent molecules, especially when two nonbonding orbitals of nitrogen atoms may take significant roles in the solute–solvent interaction, possibly in a benzene matrix. Notably, the assignment for the 534 cm^{-1} band, especially in the benzene matrix (Figure 3 in ref. [11]), seems to be less convincing, since there are a couple of peaks in the 530 – 570 cm^{-1} region that can be correlated to the 534 cm^{-1} band with an equal chance. The deuteration effect on the 373 cm^{-1} band^[28] is somewhat puzzling. However, it should be noted that the nuclear displacement of the $6b$ mode is mainly concentrated on two nitrogen atoms of the ring, thus leading to the in-plane distortion (Figure 2). For in-

stance, *ab initio* calculation (DFT; UB3LYP/6-311G(d,p)) gives calculated $6b^+$ vibrational frequencies of 565 and 557 cm^{-1} for pyridazine $^+$ - h_4 and pyridazine $^+$ - d_4 , respectively, which are very close to each other as expected. Considering the fact that the normal mode is defined at the minimum of the potential, this theoretical calculation suggests that the H/D substitution effect on the $6b$ mode could be small. It might be more surprising if two different electronic origins remain the same on H/D substitution, from the consideration of the change of zero-point energies associated with two different upper electronic states. The previous study of pyridazine methane and ammonia clusters in the gas phase by Wanna and Bernstein^[30] is more consistent with the model suggested in this work.

3. Conclusions

The conventional concept that strong interactions of two non-bonding orbitals in pyridazine induce complete electronic delocalization in the excited state is found to be not perfectly valid. This work demonstrates that the MO concept that is widely employed in the excitation and ionization spectroscopy of many molecules could mislead the detailed interpretation, especially in terms of symmetry selection rules associated with the molecular structure. For the pyridazine case, MATI spectroscopy serves as a useful tool to clarify such confusions. A high-level theory of electronic correlation, such as the EOM–CCSD theory, is also indispensable for further unambiguous understanding. Even though the vibronic coupling model by Fischer and Wormell^[6] might also be useful for the explanation of the MATI experimental results, at least for some low-frequency bands, our high-level theoretical result, which matches very well with experiments, strongly suggests that the alternative model of the in-plane distorted S_1 structure is more convincing for the pyridazine molecule.

Experimental Section

Experimental conditions have been given in detail elsewhere.^[31,32] Briefly, pyridazine (Aldrich) heated at 80°C was mixed with Ar carrier gas before being expanded into a vacuum through a 0.5 mm -diameter nozzle orifice. The supersonically cooled jet was skimmed through a 1 mm -diameter skimmer and then overlapped with two independently tunable laser pulses. The third harmonic output of a Nd:YAG laser (Spectra-Physics, GCR-150) was used to pump a dye laser (Lambda-Physik, Scanmate II) to generate the laser output in the 360 – 372 nm range. This laser pulse was used for molecular excitation. The other laser output independently tunable in the 219 – 229 nm range was generated by frequency doubling of the visible output of another dye laser (Lumonics) pumped by 355 nm of the other Nd:YAG laser (Continuum, Surelite II), to be used for ionization of excited molecules. The laser wavelength was calibrated within $\pm 0.5\text{ cm}^{-1}$ by using the optogalvanic signal from a hollow-cathode lamp (Ne). Two laser pulses were overlapped with the molecular beam in both space and time to ionize pyridazine molecules by the $(1+1)$ R2PI process. Molecular ions were repelled, accelerated, and drifted along the field-free region until they were detected by a multichannel plate (MCP, Jordan) to give the R2PI signal, which was monitored as a function of the UV excitation wavelength. For obtaining MATI spectra, molecules excited to

high-*I* Rydberg states were allowed to stay for a few microseconds in the presence of the spoil field of $\approx 2 \text{ V cm}^{-1}$, which was intentionally used to remove directly formed ions from the probing zone before they were ionized by the pulsed electric field of $20\text{--}120 \text{ V cm}^{-1}$. Pulsed-field-ionized ions drifted in the field-free region and were detected by the 25-mm-diameter dual MCPs (Jordan). The resultant signal was digitized by an oscilloscope (LeCroy) and stored in a personal computer, which also controlled two dye lasers and homemade autotracker for frequency-doubling crystals.

Acknowledgements

This work was supported by KOSEF (M10703000936-07M0300-93610 and R01-2007-000-10766-0), SRC (R11-2007-012-01002-0), and KISTI Supercomputing Center (KSC-2007-S00-2010).

Keywords: ab initio calculations • electronic structure • ionization • pyridazine • transition states

- [1] R. Hoffmann, *Acc. Chem. Res.* **1971**, *4*, 1, and references cited therein.
[2] M. Riese, J. Grotemeyer, *Anal. Bioanal. Chem.* **2006**, *386*, 59.
[3] M. P. Fülcher, K. Andersson, B. O. Roos, *J. Phys. Chem.* **1992**, *96*, 9204.
[4] D. A. Kleier, R. L. Martin, W. R. Wadt, W. R. Moomaw, *J. Am. Chem. Soc.* **1982**, *104*, 60.
[5] W. R. Wadt, W. A. Goddard III, *J. Am. Chem. Soc.* **1975**, *97*, 2034.
[6] G. Fischer, P. Wormell, *Chem. Phys.* **2000**, *257*, 1, and references cited therein.
[7] J. E. Del Bene, J. D. Watts, R. J. Bartlett, *J. Chem. Phys.* **1997**, *106*, 6051.
[8] J. Zeng, N. S. Hush, J. R. Reimers, *J. Am. Chem. Soc.* **1996**, *118*, 2059.
[9] K. K. Innes, I. G. Ross, W. R. Moomaw, *J. Mol. Spectrosc.* **1988**, *132*, 492.
[10] M. Terazima, S. Yamauchi, N. Hirota, O. Kitao, H. Nakatsuji, *Chem. Phys.* **1986**, *107*, 81.
[11] H. Li, W. Kong, *J. Chem. Phys.* **1998**, *109*, 4782.
[12] E. Ueda, Y. Udagawa, M. Ito, *Chem. Lett.* **1981**, 873.
[13] A. E. W. Knight, C. S. Parmenter, *Chem. Phys.* **1976**, *15*, 85.
[14] Y. Matsumoto, S. K. Kim, T. Suzuki, *J. Chem. Phys.* **2003**, *119*, 300.
[15] M. H. Palmer, I. C. Walker, *Chem. Phys.* **1991**, *157*, 187.
[16] K.-W. Choi, D.-S. Ahn, S. Lee, H. Choi, K.-K. Baeck, S.-U. Heo, S. J. Baek, Y. S. Choi, S. K. Kim, *ChemPhysChem* **2004**, *5*, 737.
[17] K.-W. Choi, D.-S. Ahn, J.-H. Lee, S. K. Kim, *J. Phys. Chem. A* **2006**, *110*, 2634.
[18] G. D. Purvis III, R. J. Bartlett, *J. Chem. Phys.* **1982**, *76*, 1910.
[19] J. F. Stanton, R. J. Bartlett, *J. Chem. Phys.* **1993**, *98*, 7029.
[20] J. F. Stanton, J. Gauss, J. D. Watts, M. Nooijen, N. Oliphant, S. A. Perera, P. G. Szalay, S. J. Lauderdale, S. R. Gwaltney, S. Beck, A. Balkova, D. E. Berholdt, K. K. Baeck, P. Rozyczko, H. Sekino, C. Hober, R. J. Bartlett, ACES-2, a product of the University of Florida, Quantum Theory Project.
[21] J. Gauss, J. F. Stanton, R. J. Bartlett, *J. Chem. Phys.* **1991**, *95*, 2623.
[22] J. F. Stanton, J. Gauss, *J. Chem. Phys.* **1994**, *100*, 4695.
[23] K. K. Baeck, J. D. Watts, R. J. Bartlett, *J. Chem. Phys.* **1997**, *107*, 3853.
[24] K. K. Baeck, *J. Chem. Phys.* **2000**, *112*, 1.
[25] Gaussian98 (Revision A.7), M. J. Frisch, G. W. Trucks, H. B. Schlegel, G. E. Scuseria, M. A. Robb, J. R. Cheeseman, V. G. Zakrzewski, J. A. Montgomery, R. E. Stratmann, J. C. Burant, S. Dapprich, J. M. Millam, A. D. Daniels, K. N. Kudin, M. C. Strain, O. Farkas, J. Tomasi, V. Barone, M. Cossi, R. Cammi, B. Mennucci, C. Pomelli, C. Adamo, S. Clifford, J. Ochterski, G. A. Petersson, P. Y. Ayala, Q. Cui, K. Morokuma, D. K. Malick, A. D. Rabuck, K. Raghavachari, J. B. Foresman, J. Cioslowski, J. V. Ortiz, A. G. Baboul, B. B. Stefanov, G. Liu, A. Liashenko, P. Piskorz, I. Komaromi, R. Gomperts, R. L. Martin, D. J. Fox, T. Keith, M. A. Al-Laham, C. Y. Peng, A. Nanayakkara, M. Challacombe, P. M. W. Gill, B. G. Johnson, W. Chen, M. W. Wong, J. L. Andres, C. Gonzalez, M. Head-Gordon, E. S. Replogle, J. A. Pople, Gaussian, Inc., Pittsburgh, PA, **1998**.
[26] The bond lengths (in pm) and angles (in degrees) of the ground pyridazine obtained by the CCSD/Basis-1 are $R(\text{C4-C5})=138.4$, $R(\text{C-C})=140.5$, $R(\text{C-N})=133.7$, $R(\text{N1-N2})=134.4$, $A(\text{C-C-C})=116.8$, $A(\text{C-N-N})=119.3$, $A(\text{C-C-N})=123.9$.
[27] M. Kasha, *Discuss. Faraday Soc.* **1950**, *9*, 14.
[28] B. D. Ransom, K. K. Innes, *J. Mol. Spectrosc.* **1978**, *69*, 394.
[29] A. D. Jordan, C. S. Parmenter, *Chem. Phys. Lett.* **1972**, *16*, 437.
[30] J. Wanna, E. R. Bernstein, *J. Chem. Phys.* **1987**, *86*, 6707.
[31] S. J. Baek, K.-W. Choi, Y. S. Choi, S. K. Kim, *J. Chem. Phys.* **2003**, *118*, 11040.
[32] S. J. Baek, K.-W. Choi, Y. S. Choi, S. K. Kim, *J. Chem. Phys.* **2002**, *117*, 2131.

Received: March 19, 2008

Published online on July 9, 2008